A Novel Pulse Echo Correlation Tool for Transmission Path Testing and Fault Diagnosis

David M. Horan Department of Electronic Engineering
Cork Institute of Technology, Cork, Ireland
Email: david.horan@cit.ie

Richard A. Guinee Department of Electronic Engineering
Cork Institute of Technology, Cork, Ireland
Email: rguinee@cit.ie

***Abstract*— In this paper a novel pulse sequence testing methodology is presented [22] as an alternative to Time Domain Reflectometry (TDR) for transmission line health condition monitoring, faultfinding and location. This scheme uses Pseudo Random Binary Sequence (PRBS) injection for transmission line testing and fault location with cross correlation (CCR) techniques to build a unique response profile, as a characteristic signature, to identify the type of fault, if any, or load termination present as well as its distance from the point of stimulus insertion. This fault characterization strategy can be applied to a number of industrial application scenarios embracing high frequency (HF) printed circuit board (PCB) and integrated circuit (IC) device operation, overhead lines and underground cables in inaccessible locations, which rely on a transmission line pathway or via common to all cases either for signal propagation or power conveyance.**

As an improved time-domain methodology PRBS enabled fault finding can be performed online at low amplitude levels for normal uncorrelated signal traffic disturbance rejection and to average out the presence of transmission link extraneous noise pickup over several PRBS cycles for the purpose of multiple fault coverage, resolution and identification. This unique troubleshooting tool is due to the perturbation of the transmission line with a special pseudonoise (pN) sequence of uncorrelated pulses of random polarity and the subsequent CCR measurement of their aggregate response at the test node input for line fault identification and localisation.

Based on the distinct spike-like attribute of the PRBS autocorrelation (ACR) function, a pre-location fault measurement relies on the relative time displacement of the device/system conditioned PRBS cross-correlated echo response from the ACR peak for accurate fault/load location and identification. This measured time translation of the correlation peaks can be subsequently used to determine the propagation delay of the reflected response from the fault/load-termination of the unit under test (UUT). This procedure not only results in fault/load parameter identification but also of the reflection transit time from the fault interface and thus the distance of the fault from the point of stimulus insertion.

In this paper a lumped parameter circuit model is presented to emulate generalized transmission line, using the well-known pSpice simulation package, for a range of known load-terminations mimicking fault conditions in a range of application scenarios encountered in practice. Numerous line behavioural simulations for various fault conditions, known apriori, with measured CCR response demonstrate the capability of and establishes confidence in the effectiveness of the PRBS test method in fault type identification and location. The accuracy of the method is further validated through theoretical calculation using known lumped parameters, fault termination conditions and link distance in transmission line simulation.

***Index Terms*— Transmission Path Testing, Fault Testing, Fault Identification, BIST, PRBS, Correlation Function.**

I. INTRODUCTION

Transmission line (Tx-Line) testing and fault finding is a well established and mature test and measurement discipline employed in the telecommunications and electrical power utilities industries to guarantee quality of signal transmission service to telephone subscribers and a stable electrical energy supply to domestic and industrial consumers. Time domain reflectometry (TDR) as a test strategy [11] [19] has formed the bedrock of this discipline for many years. TDR has been instrumental in the development of high frequency test and measurement calibration analysers for transmission link characterization, balance and performance optimisation in a range of HF industrial applications encompassing IC [14] and PCB design layout [17] for minimization of via/track parasitics. However if suffers from the drawback [11] [19] in that it relies on a single pulse echo strategy for transmission line fault location which is susceptible to measurement inaccuracy as a result of link attenuation with fault distance and phase change distortion with frequency as well as measurement resolution uncertainty in the presence of noise pickup.

The alternative improved strategy proposed in this paper is the application of a bipolar PRBS stimulus, which consists of a random time arrangement of pulses, resulting in a sustained pulse echo sequence with an accumulated CCR response build-up, which overcomes the difficulty of uncorrelated link noise, at low pulse energy-to-noise ratio conditions, in fault location measurement. This stochastic method, which is a well-known system identification tool [9] [10] [18] in optimal control, can also be used via cross correlation of the input PRBS stimulus with the fault echo response, over several PRBS cycles in averaging out noise pickup and normal signal traffic in the online mode, to identify the nature or characteristic signature of the fault.

The ever increasing scale in and demand for multimedia data processing applications in mobile handheld units [16] and desktop PCs has resulted in the accelerated development of high speed digital circuit architectures and CPU designs with minimum circuit feature sizes on a sub-micron scale. This continual reduction in feature size implies significantly higher device switching speeds for ultra high-speed bus designs and faster circuits $(> 1GHz)$ which necessitate improved signal path impedance and coupling control to satisfy voltage and timing budgets. As a result transmission line interconnect structures at chip, multichip, package and board level constitute one of the most critical parts for the signal integrity of all electronic systems with progressive device miniaturisation. Besides IC chip and SMT board functional testing, it is critical that all the interconnects on multilayer PCBs and IC metallization signal pathways or vias are tested for open circuit and short circuit along with delay faults in circuit operability at rated speeds [14] due to manufacturing imperfections in addition to line impedance and propagation velocity measurements. Furthermore the evolution and pervasiveness of ad-hoc wireless networks, for example bluetooth, with RF sources operating at $\sim 2.4GHz$ posses ever greater challenges to mixed signal automated test equipment (ATE), in which TDR is the mainstay, to test signal paths in UUTs at rated speeds [14].

The present recommended industrial approach [14] [17] to implementing transmission line tests and measurements, to achieve PCBs with $\pm 10\%$ impedance variation, is based on TDR. The difficulty of time-domain analysis of structures with frequency dependent parameters using TDR, in the presence of noise, is a major challenge in testing inter connects over short signal paths at high frequencies which means careful attention to bus design trace geometry in order to develop proper test procedures [17].

However PRBS perturbation is already used as a Built-In Self Test (BIST) feature for digital circuit functionality testing [6], and can be easily incorporated in any application using a simple feedback shift register, by generating a cyclic redundancy check code (CRC) as a signature of operability [15]. As such it can thus be easily used for signal path testing in such circuits and PCBs for fault identification and location, as proposed here, as well as catering for the additional measurement requirements of transmission link impedance termination and propagation velocity.

In this paper the novel application of the PRBS perturbation method of transmission line testing for fault location with identification is presented [20]. A lumped parameter *T-section* equivalent circuit model is employed to simulate per unit distance distributed generalised transmission line behaviour, using the pSpice simulation package [13], for a range of known load-terminations mimicking fault conditions encountered in practice. A unit length T-section can be suitably scaled to the required dimensions for appropriate application to overhead and underground transmission lines and to cater for PCB designs and IC devices, with sub micron pathway feature sizes, at high frequency. Numerous line behavioural simulations for various fault conditions with measured response CCR demonstrate the effectiveness of the PRBS test method in fault type identification and location. The accuracy of the method is validated through theoretical calculation using known lumped parameters, fault termination conditions and distance in transmission line simulation.

II. Overview of TDR and PRBS Testing

The current standard method of fault-finding and trouble-shooting in signal and power transmission line systems is TDR, which is a pulse echo method of fault pre-location [11] [19]. This well-known technique is used for locating faults in remote long distance overhead transmission lines and in inaccessible underground cables. TDR works on the same principle as radar in that a single pulse of energy is transmitted down a cable and when the pulse reaches the end of the cable, or a fault along the cable, part or all of the pulse energy is reflected back to the TDR test instrument. Because the velocity of propagation along the line, which is assumed homogeneous, is considered constant the time taken for the pulse to return from the fault/load-termination is a measure of distance to the source of the fault reflection interface. The TDR instrument displays the information as a waveform and/or distance reading. TDR, however, is not a perfect fault location technique because the transmitted pulse is progressively broadened and made less sharp as it propagated down the line as a result of pulse conditioning/distortion due to the frequency dependent phase change coefficient β in transmission systems [1] [4]. The aspect of pulse width is an essential feature in TDR measurement resolution in that narrow pulses give rise to very sharp trace features that are ideal for measurement. These narrow pulses are quickly attenuated with signal path frequency response rolloff because of the finite pulse energy distribution over wide bandwidth, due to pulsewidth-bandwidth reciprocity relationship [2], which results in loss of reflected pulse amplitude definition. Furthermore the susceptibility of a single attenuated pulse echo to the stochastic interference effects of extraneous noise pickup, induced in the transmission link, results in a low energy pulse echo-to-noise ratio that causes uncertainty with accompanying inaccuracy in the determination of the fault/load-termination distance. Consequently narrow pulse TDR is useful over short distances only.

Alternatively, the application of a wide pulse stimulus in TDR produces phase related wider and more rounded echo trace features, whose start points are difficult to discern as a leading edge reference for echo pulse propagation delay measurement, which results in inaccurate resolution of transmission link fault distance. However, these wide pulse stimuli are not so quickly attenuated and therefore travel further which makes them useful for long distance transmission link fault measurements. The half height pulse widths produced by commercially available TDRs vary from 2 nanoseconds to several microseconds [11]. However the TDR pulse echo technique is susceptible to the corruptive interference effects of inductively coupled link noise, which can potentially mask out weak reflections from long distance faults [11], with a resultant loss of pulse definition for accurate pulse transit time measurements for fault location evaluation. Although pulse stimuli can be repeatedly sent in cascade they are uncorrelated, since all the reflected fault information is contained in isolated unconnected pulse echoes, in contrast to a PRBS stimulus, which renders pulse stream insertion unproductive in noisy transmission link measurements.

The alternative application of PRBS perturbation to identify a transmission line fault and its location does not involve a single pulse as in TDR but a random coded bipolar series of interconnected highs and lows which are reflected by an impedance mismatch as a correlated magnified latent response distributed over the entire pN sequence. Calculating the cross-correlation of the reflected fault response with the incident PRBS and comparing its peak value time displacement with the peak autocorrelation of the incident PRBS can identify the location of fault. The amplitude profile/shape of the cross-correlated echo signal response provides a characteristic analog signature, which identifies the type of fault that is analogous to the digital CRC associated with digital circuit testing. To average out the effects of noise [9] [18] on the line, the fault response correlation can be carried out over an integral number of sequences [9], which reduces the inductively coupled noise and accentuates the fault signature with each PRBS cycle of correlation. In this way a magnified picture of the fault can be built up over a number of PRBS lengths, dramatically reducing the debilitating effects of noise.

III. Transmission Signal Path Modeling, Simulation and Testing

A continuous open twin wire configured or enclosed co-axial transmission line can be modeled by a lumped parameter *T-section* equivalent circuit as shown in Fig. 1 at low frequencies [4] [1]. This consists of a uniformly distributed series inductance *L*, resistance *R* and a shunt capacitance *C* in parallel with a conductance *G* over elemental transmission distance *dz*. If the distributed transmission line segment is less than $\frac{1}{10}$ of the operating transmission wavelength λ, it can be replaced with a lumped element equivalent circuit. A unit length T-section can be suitably scaled to the required dimensions for appropriate application to overhead and underground transmission lines and to cater for PCB designs and IC devices, with sub micron pathway feature sizes, at high frequency. The unit length model can be considerably simplified for approximation of transmission line operation at high angular frequency ω with the elimination of the distributed resistance and conductance in accordance with the condition [4]

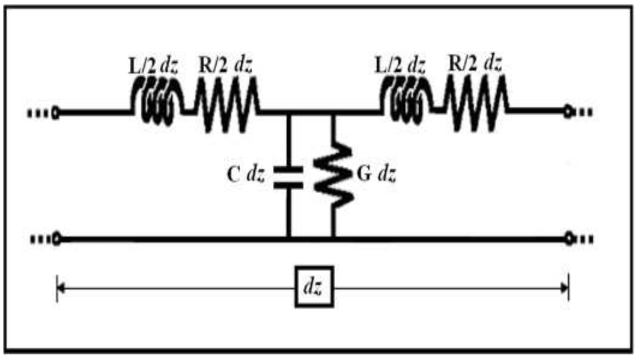

Fig. 1. Full Model Lumped Section

$$\omega L \gg R \quad and \quad \omega C \gg G \tag{1}$$

The transmission model is simulated below at low and high frequency operation for various types of line faults, known apriori, with PRBS injection in order to gauge the accuracy of the CCR process in identifying the type of fault and its location for each test case.

A. Low Frequency Line Operation - Full Model Implementation

Consider a transmission line operating at frequency 5000rads/sec and whose lumped parameter values per-loop-km are: $R = 10.15\Omega L = 3.93mHG = 0.29\mu SC = 0.00797\mu F$. A lumped section representing a 1km unit length is shown in Fig. 2. Longer lengths of line are achieved by cascading multiple sections together. The well-known characteristic impedance Z_0 and complex propagation coefficient γ for the "unit length" model in Fig. 1 are given respectively by [4] [1]

$$Z_0 = \sqrt{\frac{(R + j\omega L)}{(G + j\omega C)}} \tag{2}$$

$$\gamma = \sqrt{(R + j\omega L)(G + j\omega C)} = \alpha + j\beta \tag{3}$$

$$\alpha = \sqrt{\frac{1}{2}\left[\sqrt{(R^2 + \omega^2 L^2)(G^2 + \omega^2 C^2)} + (RG - \omega^2 LC)\right]} \tag{4}$$

$$\beta = \sqrt{\frac{1}{2}\left[\sqrt{(R^2 + \omega^2 L^2)(G^2 + \omega^2 C^2)} - (RG - \omega^2 LC)\right]} \tag{5}$$

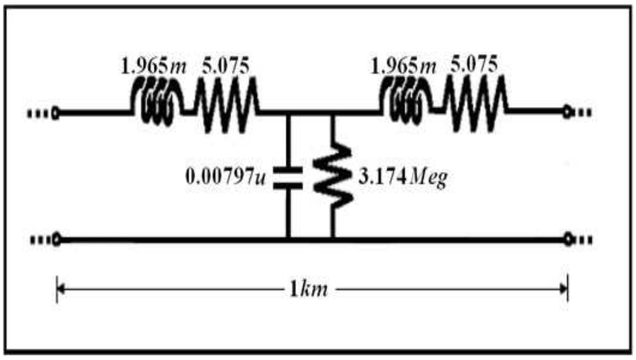

Fig. 2. Lumped Section of Test Line

The propagation coefficient for the above line parameters *per km* is $\gamma = \alpha + j\beta = 0.00712.0 + j0.0288$ where α is the attenuation coefficient in *nepers/km* and β is the phase-change coefficient in *rads/km*. The velocity of propagation is derived from the frequency of operation, which in this case is 5000 *rads/sec*, and the phase-change coefficient as follows;

$$v_p = f.(\frac{2\pi}{\beta}) = \frac{\omega}{\beta} = 173611.11km/s \tag{6}$$

B. High Frequency Line Operation - Reduced Model Implementation

Consideration of a high frequency (HF) line in accordance with (1) results in a "lossless line" with $\alpha = 0$. The real characteristic impedance Z_0 and propagation coefficient γ, as the phase change coefficient β, are given respectively by

$$Z_0 = \sqrt{\frac{L}{C}} \tag{7}$$

$$\gamma = j\beta = j\omega\sqrt{LC} \tag{8}$$

If, for example [12], a HF line is $100m$ long and operated at $20Mhz$, with $\lambda = 5.1862m$ and a characteristic impedance of 30Ω, the frequency is high enough to assume that $\omega L \gg R$ and $\omega C \gg G$, such that the line is considered lossless. The pSpice distributed model pspice97 illustrated in Fig. 3 was employed in this instance as the values of the *L* and *C* components for a lumped section are in the *pico* and *femto* range, and as such, the section would represent a very small length. The velocity of propagation is easily determined as

$$v_p = \lambda \times f = 103724km/s \tag{9}$$

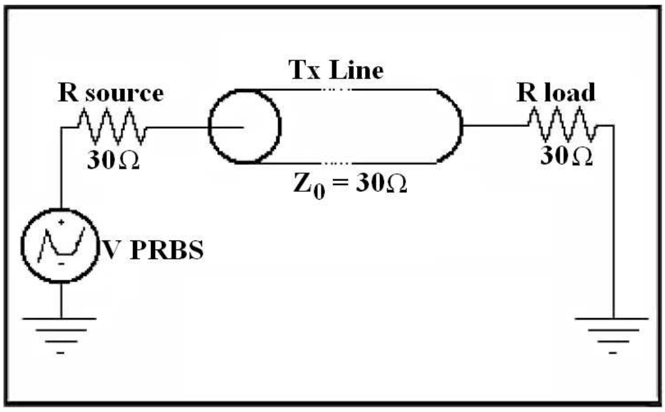

Fig. 3. HF Distributed Transmission Line Model

C. Pseudo Random Binary Sequence Injection

The PRBS stimulus is a pulse sequence which changes state in a pseudo random manner between voltage levels +a or a at discrete intervals of time, known as the chip time, Δt. The sequence is generated by a Linear Feedback Shift Register (LFSR), of length *n*, employing a primitive irreducible feedback polynomial [3] [5] [8]. A maximal length sequence N is produced, with $N = 2^n - 1$, which is periodic with temporal cyclicity $T = N\Delta t$. By virtue of its randomness statistics [3] [9] the PRBS sequence has a unique spike-like ACR function [21]over one period $N\Delta t$ as shown in Fig. 4.

The PRBS-ACR expresses the measure of expected interdependency or degree of "likeness" between a cyclically time-shifted version of the sequence with itself. The ACR metric $\varphi_{xx}(k)$, for a PRBS time function evolution shown in Fig. 5 as

$$X(t) = \{x(1), x(2), \ldots, x(j), \ldots, x(N)\} \tag{10}$$

at instants $t = j\Delta t$ with $1 \leq j \leq N$, is given by (11) for a time shift $\tau = k\Delta t$ with $0 \leq k \leq (N-1)$ between the sequences.

$$\varphi_{xx}(k) = \frac{1}{N}\sum_{j=1}^{N} x(j)x(j-k) = \begin{cases} +a^2 & \text{if } k = 0 \\ -\frac{a^2}{N} & \text{if } k \neq 0 \end{cases} \tag{11}$$

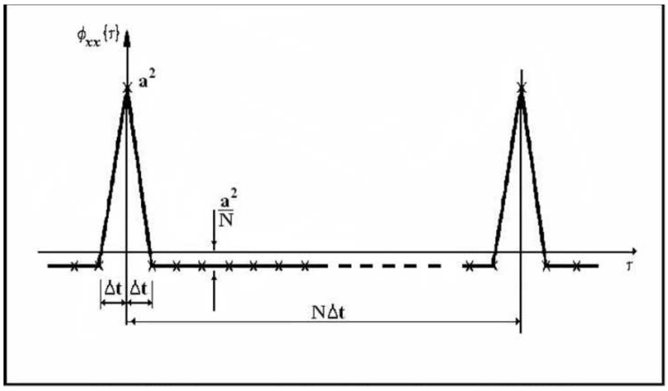

Fig. 4. Autocorrelation Function of PRBS

The ACR reduces to a triangular spike, as shown in Fig. 4, with logic bit amplitude assignment Logic $1 \rightarrow +a$, Logic $0 \rightarrow -a$. This ACR function is used in conjunction with the cross correlated echo response, reflected from a line fault termination, to determine the transit time delay and thus the fault distance.

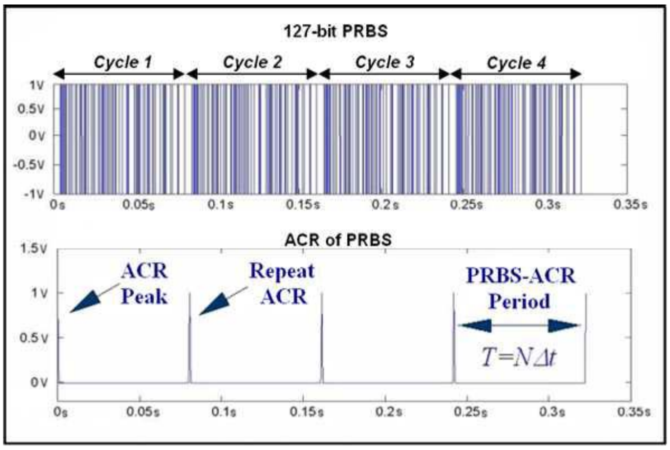

Fig. 5. 127-bit PRBS with ACR over 5 PRBS Periods

IV. Fault Diagnosis

It is well known that when a transmission line is terminated in any load Z_L other than the characteristic impedance Z_0, a reflected wave $X_r(t)$ as well as an incident wave $X_i(t)$ will be present at any point on the line as a result of a discontinuity or impedance mismatch $(Z_L \neq Z_0)$ on the line. The extreme cases of line mismatch are a shunt path, manifested as a short circuit fault $(Z_L = 0)$, and a series path disconnect which duplicates an open circuit fault $(Z_L = \infty)$. Besides the above standard "end of line" faults, other types of line characteristics, manifested as partial discontinuities, can give rise to reflections as a result of impedance mismatch. These include [11] cable joints, splits and faults due to waterlogged zones, all of which are characterised as minor mismatches. The reflected wave will be some proportion multiple of the incident wave, which is determined [1] by the reflection coefficient ρ at the load termination Z_L. If the line is terminated in some arbitrary load

Z_L other than Z_0 then the reflection coefficient and voltage standing wave ratio (VSWR) s are given, respectively, by

$$\rho = \frac{Z_L - Z_0}{Z_L + Z_0} \quad (12)$$

$$s = \frac{1 + |\rho|}{1 - |\rho|} \quad (13)$$

with $-1 \leq \rho \leq 1$. There are four general cases of line termination possible that directly influence the measured values [1] [4] of ρ and s and thus provide an indication of the type of fault, if any, or load termination present.

1) For a properly terminated or matched line, $Z_0 = Z_L$, no reflection occurs so that $\rho = 0$ and $s = 1$.
2) For an open-circuited line, $Z_L = \infty$, the entire incident wave is reflected back without phase reversal so that $\rho = 1$.
3) For a short-circuited line, $Z_L = 0$, the incident wave is reflected back with phase reversal so that $\rho = -1$.
4) For a terminated load mismatch, $Z_L \neq Z_0$, the reflected wave, will either undergo phase reversal or remain in phase with respect to the incident wave depending on the relative sizes of Z_L and Z_0. If $Z_L < Z_0$, then $\rho < 0$ and $s = \frac{Z_0}{Z_L}$. Alternatively if $Z_L > Z_0$, then $\rho > 0$ and $s = \frac{Z_L}{Z_0}$.

The phase relationship of the reflected response with the incident excitation through ρ in the PRBS-CCR process, described below, along with the measurement of s provide a direct indication of the type of load termination present. If a faulty transmission line is excited with an incident PRBS signal

$$X_i(t) = \{x_i(1), x_i(2), \ldots, x_i(j), \ldots, x_i(N)\} \quad (14)$$

the fault conditioned reflected PRBS signal response

$$X_r(t) = \{x_r(1), x_r(2), \ldots, x_r(j), \ldots, x_r(N)\} \quad (15)$$

at the sampling instance $j\Delta t$ for $j = 1, 2, \ldots, N$, will also be present on the line due to impedance mismatch. If the cross-correlation function, defined as

$$\varphi_{x_i x_r}(k) = \frac{1}{N}\sum_{j=1}^{N} x_i(j) x_r(j-k) \quad (16)$$

is applied to the incident $X_i(t)$ and reflected PRBS echo signals $X_r(t)$, a correlation peak will occur at some point in time, $k\Delta t$, as shown in Fig. 7 for an open circuit fault, which is representative of the distance l of the line fault from the point of input test stimulus application. To measure the CCR time displacement τ_l a reference point is needed, as shown in Fig. 7, which is supplied by the ACR of the incident PRBS in (11). The relative distance between these two peaks, measured in seconds, is the time τ_l taken for the PRBS perturbation to travel to and from the line fault and therefore when divided by two and multiplied by the line propagation velocity v_p will give the distance l to the source of reflection as

$$l = \frac{\tau_l}{2} \times v_p \quad (17)$$

A. High Frequency Line Fault Diagnosis

If the HF transmission line described in section III-B is considered as a simulated test case example, for various discontinuities, an illustrated fault diagnosis concerning the nature and location of the fault can be inferred as follows from the CCR response of the PRBS stimulus. In this example both open circuit (o/c) and short circuit (s/c) termination faults are considered using a simulation time step size of $\frac{\Delta t}{10}$, for an $N = 127$ bit PRBS injection at a frequency of $f_{PRBS} = \frac{1}{\Delta t} = 20Mhz$ corresponding to the reciprocal of the PRBS bit/chip duration Δt. The reference peaks are generated via the autocorrelation of the incident PRBS, which can be carried out directly at the source of stimulus. Because the PRBS is periodic in *N* with period *T*, the reference peaks repeat every $T = \frac{N}{f_{PRBS}} = N\Delta t = 6.35\mu s$, as shown in Fig. 5 and Fig. 7, which allows a maximum delay of $6.35\mu s$ to be measured before CCR overlapping occurs with the repeat ACR in Fig. 7.

If the line is terminated with an o/c fault then the entire incident PRBS stimulus is bounced back to the source without phase reversal. The conditioned waveform now present at the line input, as shown in Fig. 6, consists of the incident and reflected components. This signal is cross-correlated with the incident PRBS and the resultant CCR peak indicates the presence of an "echo" response via (16) as a signature of the line fault presence. The displacement of the CCR peak

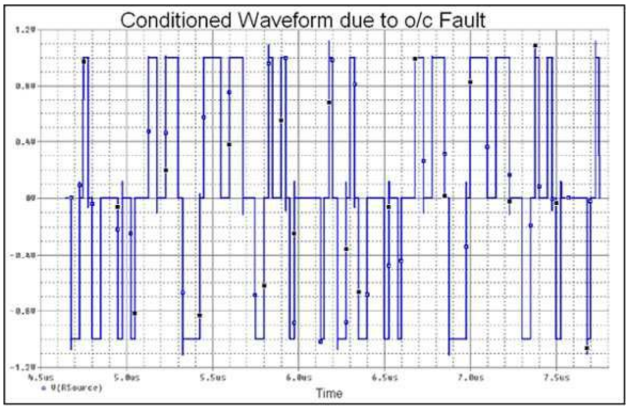

Fig. 6. Conditioned waveform on O/C Tx-line at source

relative to the ACR maximum, in Fig. 7, is a measure of the propagation delay for the PRBS test signal disturbance to traverse the line twice, that is, from the input stimulus point to the fault interface and back with a distance coverage of *2l*. The measured displacement of $\tau_l = 1.9282\mu s$, ascertained from the relative positions of CCR and ACR peaks, is an accurate gauge of the o/c fault location at the end of a $100m$ HF transmission line. This can be verified from simple theoretical considerations using (17) to give $l = \frac{\tau_l}{2} \times v_p = 0.964\mu s \times 103724km/s = 100m$ where l is the fault distance. Therefore knowledge of the CCR peak displacement τ_l and link propagation velocity v_p is all that is required to estimate the fault location l.

Alternatively if the line is terminated with a short circuit fault at a distance of $100m$ the PRBS echo response will

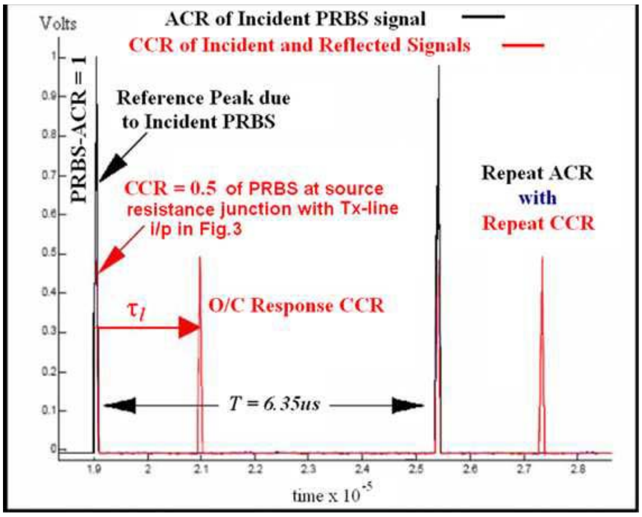

Fig. 7. ACR and CCR Functions for O/C Fault Conditions over 2 PRBS Cycles

undergo phase reversal upon reflection. Cross-correlation of the reflected waveform with the incident PRBS stimulus results in two peaks in Fig. 8 corresponding to the input PRBS-ACR and the response CCR via (16). The response CCR peak is negative in this instance due to phase reversal and occurs at the same point in time in Fig. 8 as for the open circuit fault condition in Fig. 7.

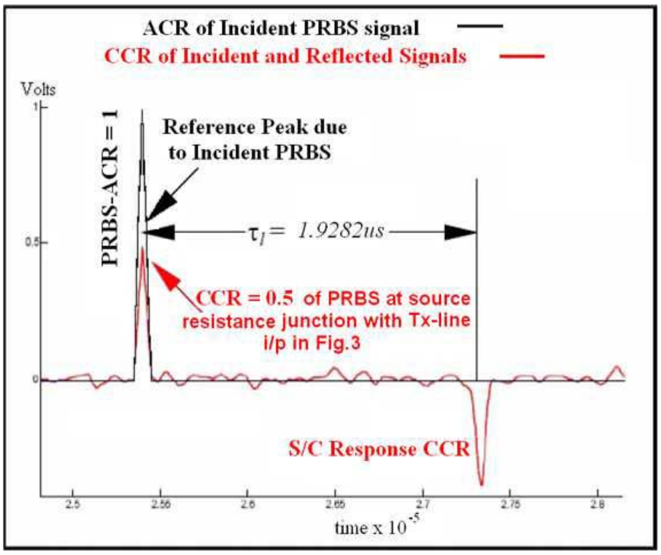

Fig. 8. ACR and CCR Functions for S/C Fault Conditions over 1 PRBS Cycles

The amplitude of the CCR peaks in Fig. 7 and Fig. 8, from the reflected PRBS echo, is below the maximum ACR reference value of 1.0 due to the source impedance matching to the transmission line ($Z_0 = R_{source}$) in Fig. 3 with a 50% input stimulus voltage drop across the source resistance R_{source}. The usefulness of the observed CCR responses in Fig. 7 and Fig. 8 is that the existence of correlated echo peaks and their polarity provides an indication of the type of line fault present. The first observation that should be made is whether or not a CCR correlation peak is evident other than the ACR at the reference locations. If there is no CCR peak present then it can be inferred that $Z_L = Z_0$, for matched conditions, as there are no reflections on the line. If, however, there is a positive peak then $Z_L > Z_0$ and a possible open circuit or high impedance fault is present. Conversely, if a negative peak is present then $Z_L < Z_0$ and a possible short circuit or low impedance fault exists on the line.

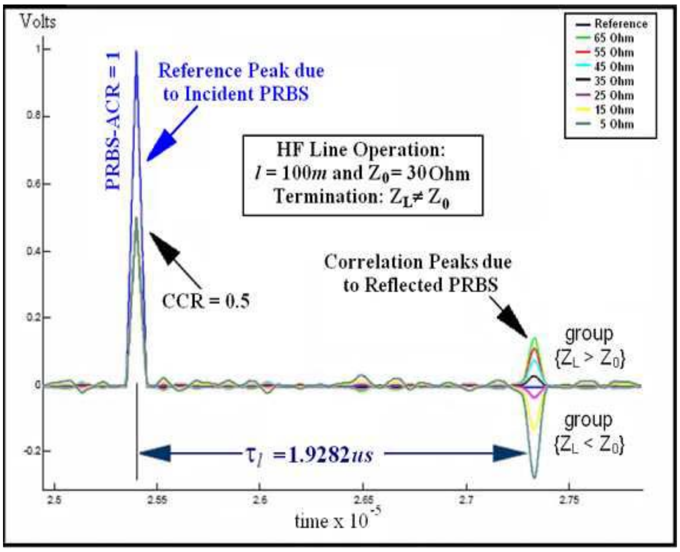

Fig. 9. ACR and CCR Functions for Fault Termination Conditions $Z_L \neq Z_0$ over 1 PRBS Cycles

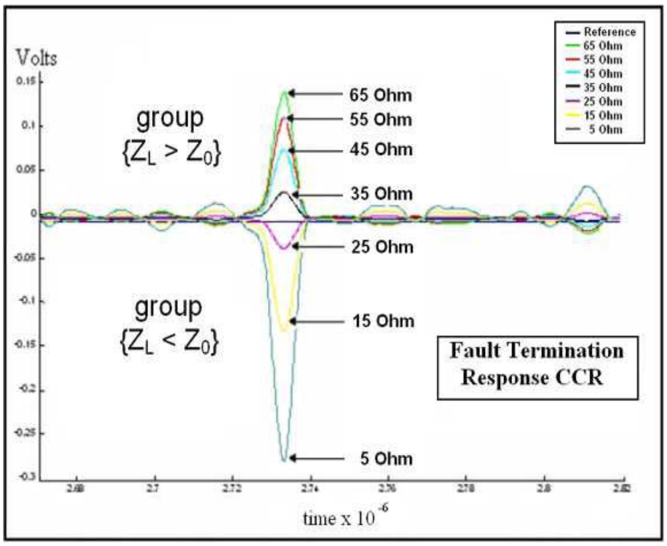

Fig. 10. Enlarged View of Response CCR in Fig.8

The presence of low or high impedance fault manifestations, other than open or short circuit types, can also be deduced from the CCR of the PRBS echo response for a range of load terminations $Z_L \neq Z_0$. Termination of the HF line with fault impedance values from 5Ω to 65Ω, in steps of 10Ω, and cross correlation of line echos reveal the existence of CCR responses with peak magnitudes and polarities commensurate with the termination values as per Fig. 9 and Fig. 10. As expected all the CCR peaks occur at the same point in time in Fig. 9 and Fig. 10, as the impedance fault remains the same distance $l = 100m$ away from the source stimulus. The amplitude of the CCR peaks varies with Z_L and the degree of mismatch with Z_0, as per the reflection coefficient ρ in (12), which is passed proportionally to the correlation peaks. If, for example, fault impedance terminations $(Z_{L1}, Z_{L2}) > Z_0$ are employed with $Z_{L2} > Z_{L1}$ then the polarities of the CCR peaks are positive in both cases. Furthermore comparison of the relative CCR peak magnitudes illustrate larger CCR amplitudes with termination value Z_L, as per Fig. 9 and Fig. 10, resulting in increased reflected echo response ρ, that is, for Z_{L1}, Z_{L2}

$$\max \varphi_{x_i x_r}\big|_{Z_{L2}} > \max \varphi_{x_i x_r}\big|_{Z_{L1}} \tag{18}$$

Similar observations hold for the converse case in Fig. 10, which depicts a negative polarity change with $Z_L < Z_0$ and increased absolute CCR value with reduced fault termination impedance. The PRBS fault location strategy can also be used to estimate the reflection coefficient ρ for a given Z_L as

$$\hat{\rho} = \frac{\max \varphi_{x_i x_r}\big|_{CCR}}{\max \varphi_{x_i x_r}\big|_{ACR}} \tag{19}$$

from the relative comparison of "reflected" CCR peak to the incident correlation peak (CCR=0.5) from the total CCR measurement, as the ratio in (19), for each of the impedance fault Z_L cases depicted in Fig. 10. This information can in turn be used to estimate the actual impedance fault manifestation Z_L from the expression

$$\hat{Z_L} = \frac{Z_0(1+\hat{\rho})}{(1-\hat{\rho})} \tag{20}$$

and the VSWR s, via (13), as

$$\hat{s} = \frac{1+|\hat{\rho}|}{1-|\hat{\rho}|} \tag{21}$$

Comparison of the reflection coefficient estimates $\hat{\rho}$ with those values ρ from theoretical considerations using (12) show a very accurate fit when plotted in Fig. 11 for various fault impedance terminations which validates the PRBS test strategy. Subsequent evaluation of the line fault impedance $\hat{Z_L}$, as per Fig. 12 and VSWR $\hat{s}$ from the above reflection coefficient estimates $\hat{\rho}$, show excellent agreement with corresponding theoretical values, for various fault impedance terminations, which further enhances confidence in the PBRS diagnostic method of fault identification

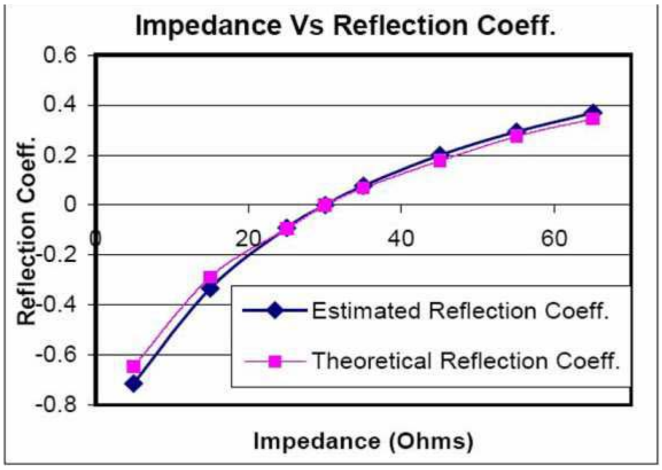

Fig. 11. Plot of Reflection Coefficient Estimates

Fig. 12. Plot of Load $\hat{Z_L}$ Estimates

B. Fault Identification of Lossy Line

If a lossy transmission line is examined attenuation of the PRBS test stimulus will occur as it propagates the line. However in contrast to the single pulse diagnostic technique, encountered in TDR, a sustained correlated response is garnered for all input pulses over the complete PRBS length resulting in a cumulative CCR echo response which is much greater than that afforded by TDR. The performance of the PRBS test method, with line attenuation, in fault location and identification can be gauged from consideration of the low frequency (LF) lossy transmission line example in section III-A through pSpice simulation [12] for an open-circuit fault condition at a distance l of $100km$. A reduction of the cross-correlation peak can be seen in Fig. 13 as a result of PRBS test stimulus attenuation. If line attenuation α is severe, to the extent that the fault signature is submerged in the noise pickup due to inductive coupling on an actual transmission (Tx) line, multiple PRBS cycle correlation can be used to rescue the echo response from the noise floor. Alternatively this well known multiple cycle correlation procedure, which is used in noisy system identification [7] [18] for parameter extraction, can also be employed at low amplitude levels for continual online Tx-line fault monitoring so as not perturb or interfere with normal uncorrelated signal traffic. However, examination of the CCR response in Fig. 13 reveals that the Tx-line fault on this line is of the open-circuit type as the cross-correlation peak has positive amplitude. The location of the fault impedance interface is again identified by the displacement of the cross-correlation peak, which is located at $2.3207ms$, from the autocorrelation peak, which is positioned at $1.17ms$. This gives a net round trip propagation delay τ_l of $1.1507ms$. The location of the fault can now be easily estimated, using (17) with the known value of v_p, as $\hat{l} = 576us \times 173611.111km/s = 100km$ which is identical to the known value l used in simulation and as such validates the PRBS test methodology for fault detection on lossy lines.

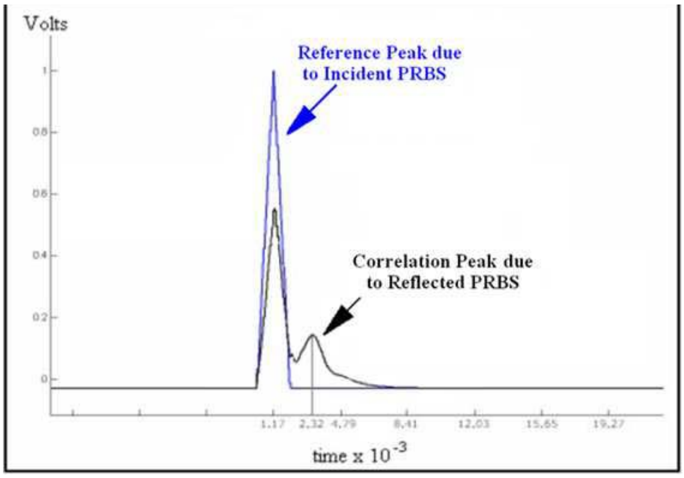

Fig. 13. Lossy Tx-Line ACR and CCR Functions for an O/C fault over 1 PRBS Cycle

Further PRBS testing for a range of lossy line fault impedance terminations yield estimates which are practically identical to those used in Tx-line simulation which further establishes concept validation.

Under matched line conditions, $Z_L = Z_0$, the PRBS based test strategy described above can be also used to estimate the attenuation coefficient α of the line, which is analytically expressed in (4) from the propagation coefficient γ in (3). If a lossy line is composed of 8 cascaded T-sections as described in section III-A, for example, and the line is operated under matched conditions with $Z_L = Z_0$, then no reflections occur on the line. The incident PRBS, as well as the output traveling PRBS wave from T-section #1 and T-section #2, which represent readings taken at 20km and 40km respectively from the source, are plotted in Fig. 14 below.

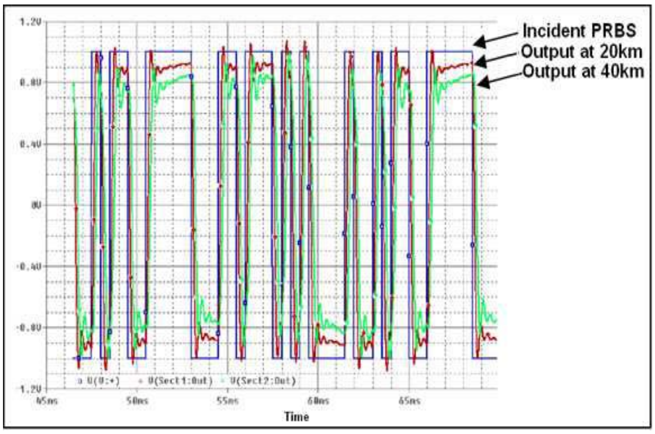

Fig. 14. Plot of Incident PRBS signal at $0km$ $20km$ and $40km$

A clear attenuation and delay is evident from Fig. 14, with both parameters increasing with line distance from the source excitation. It is difficult to measure both these parameters accurately from Fig. 14, as a particular reference point is required as in TDR. PRBS excitation negates this problem, however, as the whole PRBS traveling wave is taken into account in the calculation of the response CCR metric at various T-section output points on the line under balanced line conditions. The resultant CCR response after each of the 8 T-sections is portrayed in Fig. 15 which illustrates a progressive delay in the CCR peak with distance, a reduction in peak amplitude with attenuation as well as CCR "pulse" broadening with phase change down the line from the source. The delay and attenuation parameters of the CCR peaks are clearly visible and measurable. The availability of an accurate α calculation is important in long distance communications where repeater positioning is necessary. An estimation of an α that is too low may result in the signal being lost between repeaters, while an estimation of too high an α may result in more repeaters than is necessary with cost implications.

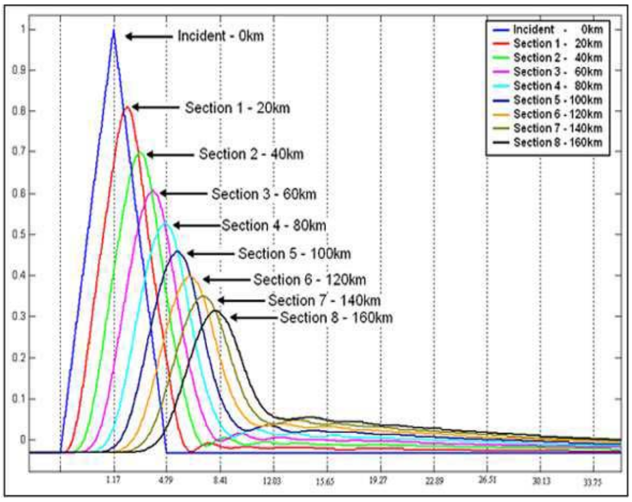

Fig. 15. CCR responses from 0km - 160km in 20km steps

The estimated value of α from Fig. 16, via PRBS testing for balanced line conditions, is in complete agreement with the theoretical value of $0.00712\ Nepers/km$ in section III-A. The graph in Fig. 16 plots the theoretical line loss in mV, as a measure of line attenuation, and the measured attenuation estimate from the decreasing CCR peak value in Fig. 15. The measured attenuation is an excellent fit validating the use of this method for an estimation of α.

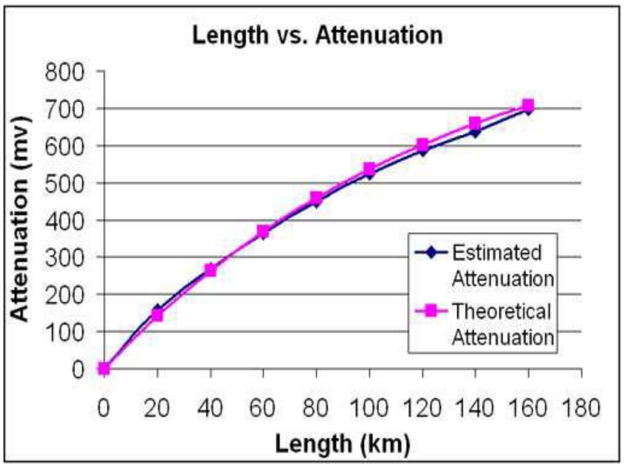

Fig. 16. Plot of theoretical and estimated attenuation

V. CONCLUSION

In this paper a novel method for fault diagnosis on transmission paths has been proposed as a competitor to the industrial TDR standard. This method relies on the unique stochastic attributes of maximal length PRBS stimuli and in particular their distinctive two-valued delta or spike-like autocorrelation function for fault location and identification. Consequently it can be used to estimate the impulse response of a faulty transmission line, in order to identify nature of the fault type and its actual location, through cross correlation of the reflected "echo" pulse stream. The echo signature of the line fault is the magnified collective response to a time arranged PRBS sequence of random pulse stimuli, propagated down the line towards the fault termination, and as such is the main advantage of using PRBS testing in preference to the single pulse method in TDR.

This novel test strategy, which is generally incorporated as a BIST feature for CPU and digital IC "health" conditioning and monitoring in complex integrated systems, has been validated via pSpice simulation of transmission line behaviour for a range of fault impedance terminations ranging from open to short circuit types. Further confidence enhancement of the method has been provided by the success in the identification of a range mismatched fault impedance terminations. Also the correlation method has been shown to give excellent estimations of the attenuation coefficient of the line under matched conditions and the reflection coefficient under mismatched conditions.

From the demonstrated effectiveness of the above simulated transmission line examples, in modelling various fault impedance termination scenarios, and established confidence in the accuracy of the correlation method in fault diagnosis it is reasonable to assume that this technique can be usefully applied to a number of industrial applications incorporating high frequency IC and PCB fault testing and characterization. This fault diagnostic tool could be deployed for troubleshooting short signal pathways as encountered in multilayered high frequency PCB cards incorporating fast CPUs and high speed digital architectures and in IC metalization pathways or vias. This method can be useful in latter case as a test aid for chip layout and characterization in "via" routing optimization, with minimum path length, to reduce the series resistance and inductance and shunt capacitance line parasitics which can cause excessive processor time critical signal propagation delays.

In summary PRBS testing can be used to determine the nature/type of fault, its location and magnitude along with the reflection coefficient and VSWR on transmission pathways in HF mixed signal systems. It can further be used to calculate the attenuation of the line under matched conditions.

ACKNOWLEDGMENT

The authors would like to acknowledge the support of the Department of Education and Science, Ireland for research funding and ERICSSON Ireland, Beech Hill, Clonskeagh, Dublin 4, Ireland for industrial support.

REFERENCES

[1] F.R. Conner, *Waves*, Arnold publishers, Great Britain, 1972.
[2] F.R. Conner, *Signals*, Arnold publishers, Great Britain, 1972.
[3] M.G. Hartley, *Digital Simulation Method*, Peter Peregrinus Ltd., England, 1975.
[4] W. Fraser, *Telecommunications*, MacDonald and Jane's Publishers, London, 1978.
[5] D. Green, *Modern Logic Design*, Addison-Wesley, England, 1986.
[6] B.R. Wilkins, *Testing Digital Circuits*, Van Nostrand Reinhold, 1986.
[7] L. Ljung, *System identification: Theory For The User*, PHI, 1987.
[8] K. Zeng, C.H. Yang , and D.Y. Wei, *Pseudorandom Bit Generators in Stream-Cipher Cryptography*, Computer, vol.24, issue 2, pp.8-17 February 1991.
[9] J. Schwartzenbach and K.F. Gill, *System Modelling and Control*, Arnold Publishers, London, 1992
[10] K. Godfrey, *Perturbation Signals for System Identification*, PHI, New York, 1993.
[11] B. Clegg, *Underground Cable Fault Location*, McGraw Hill, England, 1993.
[12] A. Vladimirescu, *The Spice Book*, J.Wiley, NY, 1994.
[13] MicoSim pSpice, Circuit Analysis Software, Ver.8.0, MicroSim Corp., June 1997.
[14] A. Grochowski, D. Bhattacharya, T.R. Viswanathanand and K. Laker, *Integrated Circuit Testing for Quality Assurance in Manufacture: History, Current Status and Future Trends*, IEEE Transactions on Circuits and Systems - II: Analog and Digital Signal Processing, Vol.44, No.8, August. 1997.
[15] R.A. Guinee, *Digital Circuit Testing with Signature Analysis Employing Pseudorandom Binary Sequence (PRBS) Generators*, Proceedings of the IASTED International Conference Applied Modelling and Simulation, Sep.1-3, 1999.
[16] M.W. Oliphant, *The Mobile Phone Meets The Internet*, IEEE Spectrum, Aug 1999.
[17] *Printed Circuit Test (PCB) Methodology User Guide*, Rev. 1.6, Jan 2000, Intel Corp. Available online at www.intel.com/design/chipsets/applnots/29817901.pdf
[18] R.A. Guinee, *Variable Speed Motor Drive Testing and Parameter Identification using Pseudorandom Binary Sequences*, IEEE-Melecon 2000, 10th Mediterranean Electrotechnical Conference, May 29-May 31, 2000.
[19] *Time Domain Reflectometry Theory*, Application Note 1304-2 for use with Agilient 86100B Infinium DCA, Agilient Technologies, Aug. 2002.
[20] D.M. Horan, *Distance Simulation using Pseudo Random Binary Sequences*, Project Report by D. Horan, Cork Institute of Technology, May 2004.
[21] D.M. Horan and R. Guinee, *Correlation analysis of random number sequences based on pseudo random binary sequence generation*, IEEE ITSOC Information Theory Workshop, pp. 76-80, 2005.
[22] D.M. Horan and R. Guinee, *A Novel Pulse Echo Correlation Tool for Transmission Path Testing and Fault Finding using Pseudorandom Binary Sequences.*, IEEE International Symposium on Defect and Fault Tolerance in VLSI Systems, pp. 229-237, 03-05 Oct. 2005.

Richard A. Guinee (M'96) received the B.E., M.Eng.Sc., and Ph.D. degrees in electrical engineering from University College Cork, Ireland, in 1975, 1977 and 2003 respectively. From 1975 - 1977 he was a research engineer at the AERE - Culham Laboratory, G.B. - involved in D2O laser detector design. From 1977 to 1981 he was involved in industry in the design of electrical controls and product development and in industrial consultancy in the design of 380V/10kV electrical installation systems. Since 1981 he has been with the Cork Institute of Technology as a lecturer in electronic engineering and digital communications systems. His research interests are in mathematical modeling and simulation of electrical motor drives, statistical information sources and spread spectrum communications systems. Contact him at rguinee@cit.ie.

David M. Horan is a Master of Engineering candidate in Electronic Engineering at the Cork Institute of Technology. His research interests include cryptography and random number genration. Horan received the BEng degree in Electronic Engineering from Cork Institute of Technology in 2004. Contact him at david.horan@cit.ie